Development of slender transport pathways in unsaturated fractured rock: Simulation with modified invasion percolation

Robert J. Glass
Flow Visualization and Processes Laboratory, Sandia National Laboratories, Albuquerque, New Mexico, USA

Michael J. Nicholl
Mining and Geological Engineering, University of Idaho, Moscow, Idaho, USA

Harihar Rajaram and Benjamin Andre
Civil, Environmental, and Architectural Engineering, University of Colorado, Boulder, Colorado, USA

Received 10 December 2003; revised 17 January 2004; accepted 2 February 2004; published 20 March 2004.

[1] Slender transport pathways have been found in laboratory and field experiments within unsaturated fractured rock. Here we consider the simulation of such structures with a Modified form of Invasion Percolation (MIP). Results show that slender pathways form in fracture networks for a wide range of expected conditions, can be maintained when subsequent matrix imbibition is imposed, and may arise even in the context of primarily matrix flow due to the action of fractures as barriers to inter-matrix block transport. *INDEX TERMS:* 1832 Hydrology: Groundwater transport; 1875 Hydrology: Unsaturated zone; 3210 Mathematical Geophysics: Modeling; 5104 Physical Properties of Rocks: Fracture and flow. **Citation:** Glass, R. J., M. J. Nicholl, H. Rajaram, and B. Andre (2004), Development of slender transport pathways in unsaturated fractured rock: Simulation with modified invasion percolation, *Geophys. Res. Lett.*, *31*, L06502, doi:10.1029/2003GL019252.

1. Introduction

[2] As a result of environmental issues associated with waste disposal in arid regions (past, present, and future), infiltration into unsaturated, fractured rock has become a high profile problem in subsurface hydrology. Experiments have shown that within individual fractures, gravity plays a first order role to create vertically extensive liquid (water) phase structures [*Nicholl et al.*, 1994; *Su et al.*, 1999]. Additionally, fractures have been found to act as capillary barriers that restrict matrix communication [*Glass et al.*, 1996]. It has been hypothesized [*Glass et al.*, 1995, 1996], that these two behaviors can combine to create transport pathways within unsaturated fractured rock that remain slender with depth. Subsequent field experiments [*Glass et al.*, 2002b] and large-scale laboratory experiments [*Glass et al.*, 2002a; *LaViolette et al.*, 2003] have confirmed the operation of local convergence mechanisms to create slender transport pathways.

[3] The formation of slender pathways in unsaturated fractured rock highlights the need to develop new conceptual models that are not fundamentally diffusive. Here, we apply an approach based on a Modified form of Invasion Percolation (MIP), a simple growth algorithm that generates phase structure through the operation of local rules that embody the physics of immiscible displacement. We identify three flow regimes within fractured rock where we pursue an MIP based analysis. Simulation results exhibit large-scale phase structure that is consistent with experiment. For time scales and fluxes where we can neglect the influence of the matrix, slender pathways form within the fracture network. Once formed, these slender pathways become surrounded by wetted zones that are limited by the action of fractures as capillary barriers to lateral flow within the matrix. For very low flow and long time scales where flow occurs primarily in the matrix, slender phase structures form even without fracture flow because of the capillary barrier action of fractures.

0094-8276/04/2003GL019252$05.00

2. MIP Model

[4] Invasion Percolation (IP) is a simple growth algorithm that generates phase structure through the operation of local rules that embody the physics of immiscible displacement within a network of pores. First introduced by *Wilkinson and Willemsen* [1983], IP has been modified (MIP) in many ways such as to bring in gravity [*Meakin et al.*, 1992; *Glass and Yarrington*, 1996; *Ioannidis et al.*, 1996], centrifugal forces [*Holt et al.*, 2003], viscous forces [*Xu et al.*, 1998], as well as capillary smoothing mechanisms in porous media [*Blunt and Scher*, 1995; *Glass and Yarrington*, 1996] and fractures [*Glass et al.*, 1998]. Recently, MIP has been applied to the movement of DNAPL within a fracture network under conditions of ambient groundwater flow [*Ji et al.*, 2003] and further modified to simulate pulsation or dripping as occurs in many buoyant-gravity destabilized flows [*Glass and Yarrington*, 2003]. For all of these situations, one can apply MIP above the pore scale in a macroscopic form [e.g., *Ioannidis et al.*, 1996].

[5] For the fracture-matrix system, we apply a simple macroscopic form of MIP that includes only capillary and gravity forces without the inclusion of redistribution during invasion (as required to consider pulsation or dripping). The simulation domain is subdivided into uniform cubes (sites) that represent either fracture or matrix. The fracture-matrix system must be discretized finely enough that fracture sites maintain the connectivity of individual fractures and separate matrix blocks appropriately. Each site is assigned a

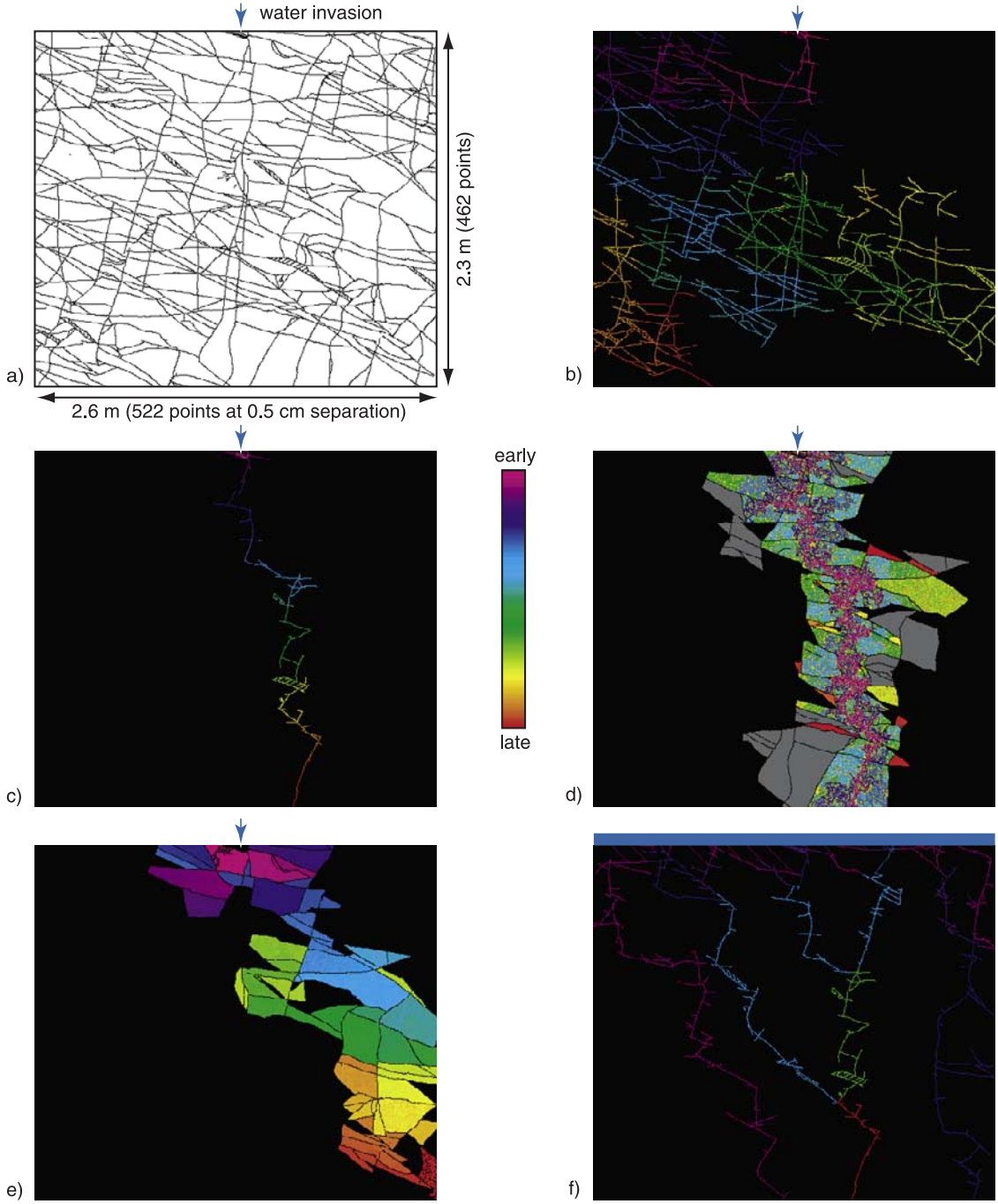

Figure 1. a) Fracture network. b) Invasion of fracture network, $B = 0$, colors represent the order of invasion, from early to late; c) Invasion of fracture network, $B = 0.0033$; d) Invasion of surrounding matrix from flowing fracture given by c), color represents pressures up to the cutoff $P_t = -66$ and gray the additional invasion with an increase to $P_t = -33$; e) Invasion of fracture-matrix network, $B = 0.033$; f) formation of convergent pathways for distributed flow (blue bar along the top boundary), color now represents the amount of convergence at a particular pathway within the network.

local capillary invasion pressure defined as the percolation threshold required to span the cube with the invading phase. These capillary invasion pressures are associated with the local mean aperture for fractures, d_f, and the local mean pore size (diameter) for the matrix, d_m, via the Laplace-Young equation. We may write the total invasion pressure, p_t, for a site as the sum of the capillary and gravitational components:

$$p_t = -\frac{2A_i\sigma\cos(\alpha)}{d_i} - \Delta\rho g z \qquad (1)$$

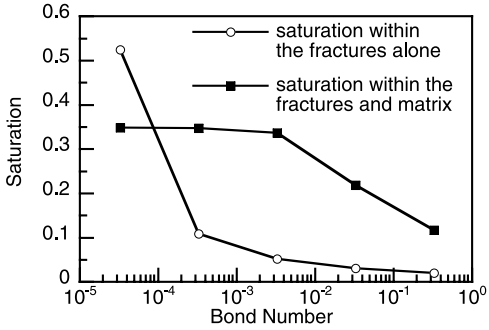

Figure 2. Volumetric fraction (i.e., saturation) of the fracture or matrix network that is invaded as a function of B. The larger B, the more slender the structure, and for our network $B > 10^{-3}$ yields the long slender ladders shown in Figure 1c.

where σ is the water-air surface tension, α the water-air-rock contact angle, $\Delta\rho$ the density difference between water and air, g the acceleration due to gravity, z the distance into the network (positive downward), and the subscript i denotes either fracture or matrix. The difference in geometry between conceptual models for fracture apertures and matrix pores (local parallel plates vs. cylindrical capillary tubes) leads to a small difference in formulation of the Laplace-Young equation, which is explicitly included by setting $A_i = 1$ for fracture sites and 2 for matrix sites. To further generalize the problem, we define the following dimensionless variables (denoted with capitals):

$$d_i = \langle d_i \rangle \quad z = \Delta z Z \quad p_t = \frac{2A_i\sigma\cos(\alpha)}{\langle d_i \rangle} P_t \quad B = \frac{\Delta\rho g \langle d_i \rangle \Delta z}{2A_i\sigma\cos(\alpha)}$$

where $\langle d_i \rangle$ is the mean value (arithmetic) of d_i for the *ith* domain, Δz is a representative macroscopic length scale over which d_i varies relative to z, and B is the dimensionless Bond number. The nondimensional total invasion pressure at a site now becomes:

$$P_t = -\frac{1}{D} - BZ \tag{2}$$

Invasion of the network is accomplished with a cycled IP algorithm. In each cycle, the algorithm searches sites connected to the fluid source and invades the one site with the lowest invasion pressure. Each act of invasion opens new sites for search in the next cycle.

3. Simulations

[6] For unsaturated flow in fractured rock, we consider three regimes where we may apply a simplified analysis with MIP. The first is for time scales and fluxes where flow will primarily occur within the fracture network and the matrix can be neglected. Second, once a phase structure is formed within the fracture network, at intermediate time scales water will move from the flowing fractures into the adjoining fracture-matrix network. Finally, when fluxes are very small and time scales are large, and invasion of the fracture-matrix network must include the concurrent participation of both fractures and matrix.

[7] A two-dimensional (2D) fracture network used in our simulations was patterned on measured data from within a 3.5 × 3.5 × 5 m tall block of welded tuff [*Glass et al.*, 2002b]. Figure 1a shows the 2.6 m wide by 2.3 m tall fracture network used in our simulations, which was discretized at 0.5 cm resolution (522 by 462 points). This network is pervasive with very few unconnected fractures and a fracture spacing that is ~10–30 cm. While a variety of aperture and pore size distributions can be considered, for simplicity, sites within the fractures and matrix were assigned d_i values (spatially uncorrelated within each) from uniform distributions with minimum values of 0 and maximum values of twice $\langle d_i \rangle$. Capillary contrast between the fractures and matrix, as defined by $\langle d_f \rangle / \langle d_m \rangle$, influences the behavior of the solution when both fractures and matrix are included. There, overlap in the distributions model contact areas between matrix blocks. For purposes of illustration, capillary contrast was kept at 1000.

[8] Our first simulations ignore the matrix, and consider the influence of B (defined with $\langle d_f \rangle$) on infiltration in the fracture network alone. Invasion began from a point source located at the center of the upper boundary, and simulations were stopped when water contacted the bottom boundary. At $B = 0$, gravity is ignored, equation (2) defaults to standard IP, and infiltration spans our pervasive fracture network both vertically and horizontally (Figure 1b). Inclusion of gravity focuses flow within the fracture network by influencing the choice of fracture site to invade. Even at small B (0.0033), we see the influence of gravity to form a slender pathway (Figure 1c). By plotting the fraction of the network invaded as a function of B (Figure 2), we see that this slender pathway structure is robust over a wide range of conditions ($B > 10^{-3}$). For infiltration into a water wettable network ($\Delta\rho \sim 1$, $\sigma \sim 72$ dynes/cm, $\alpha \sim 0°$) this result suggests that slender infiltration structures will form in our network for the product $\Delta z \langle d_f \rangle > 10^{-4}$ cm^2. Thus, for $\langle d_f \rangle$ of order 0.01 cm, slender pathway structures will form for Δz greater than 0.01 cm corresponding to a scale model of our network that is 5.22 cm by 4.62 cm or larger.

[9] Once a slender pathway has formed within the fractured rock, we can consider intermediate time scales where water imbibes from the flowing fractures into the surrounding matrix. For this analysis, we neglect the influence of gravity ($B = 0$). Taking Figure 1c as our inflow source, adjacent matrix sites are invaded using the IP algorithm until all sites with P_t below a specified cutoff have been invaded. Nonflowing fractures (large d) act as barriers to invasion. Because of this contrast, matrix blocks will fill to near saturation before fluid crosses a non-flowing fracture to enter another matrix block. Additionally, only one site within the fracture will be filled when the fracture is crossed. If none of the sites within a fracture have an entry pressure less than the cutoff pressure, invasion is blocked. By acting as capillary barriers to flow, the non-flowing fractures restrict lateral growth of the wetted zone. For illustrative purposes, we show wetting at two arbitrary values of cutoff P_t in Figure 1d: $P_t = -66$ (color) with further wetting to $P_t = -33$ (dark gray).

[10] Finally, we consider very low flow rates and long time scales where the invasion of the fracture-matrix network will be controlled by both fractures and matrix. From the same

point source as in Figure 1c but with both fracture and matrix sites active, we varied B (defined with $\langle d_f \rangle$ for consistency). Invasion was continued to breakthrough at the bottom of the system. In this regime (Figure 1e), fractures act as barriers to flow. Water moves immediately into a matrix block from the point source, fills that block, and then seeks out a breaching point (smallest P_t) in the surrounding fractures. Water crosses the fracture at the breach point, enters the next matrix block and the process is repeated. Gravity biases the selection of breach points to be lower within the entire wetted structure and thus influences the choice of matrix blocks that are invaded. The shape of the large-scale phase structure becomes entirely dependent on the properties of the fractures. The larger B, the more slender the structure, as is emphasized in a plot of the volume fraction of matrix invaded (Figure 2).

4. Discussion and Conclusion

[11] We applied MIP to simulate slender pathway formation within unsaturated fractured rock in context of three flow regimes. In each regime, we find slender pathways to form and be maintained. For time scales and fluxes where unsaturated flow within the fracture network is dominant, slender phase structures occur over a wide range of Bond number. Once these slender pathways form, a limited surrounding wetted zone develops at longer time scales where matrix interaction becomes important. There, lateral matrix flow is limited by the action of fractures as capillary barriers. For very low flow rates and long time scales, fracture flow is negligible with respect to that in the matrix. However, matrix flow is constrained by capillary barriers (dry fractures) to again be slender, the degree to which is dependent on the capillary properties of the fracture network, not the matrix.

[12] MIP results are qualitatively similar to expectations in natural unsaturated fractured rock formations. There, field evidence [*Glass et al.*, 2002b], laboratory experiments [*Glass et al.*, 2002a; *LaViolette et al.*, 2003], and fundamental physics [*Glass et al.*, 1995, 1996] all point towards the formation of slender pathways that limit interaction between the flowing fluid and surrounding rock mass. The physical processes that work to keep pathways slender (capillary barriers, gravity-driven fingers) are by nature discrete, and thus conform well to the MIP approach. For example, if we consider the influence of distributed flow into the fracture network, MIP yields convergence within the fracture network with depth as illustrated in Figure 1f. While the network used in our simulations contains a set of fractures dipping gently to the right that influence the merger process, MIP will yield merger within any network topology once pathways cross.

[13] The success of the simple MIP analysis presented here warrants further investigation. With the current approach, critical analyses can consider: aperture/pore distributions and overlap (i.e., contact areas) between the fracture and matrix on slender pathway formation; network topology and property distributions in 2D or 3D on depth of convergence; as well as the simulation of nonwetting fluid migration such as DNAPL below the water table in saturated fractured rock. More sophisticated MIP based approaches can also be applied to consider the influences of so far neglected processes such as vapor phase transport, film flow, and mineral dissolution and precipitation. Lastly, MIP provides a means of exploring the possibly special behavior at fracture intersections imposed by their local geometry.

[14] **Acknowledgments.** This work was funded by U.S. Department of Energy's Basic Energy Sciences Geoscience Research and Environmental Management Science Programs under contract DE-AC04-94AL85000 at Sandia National Laboratories, DE-FG07-02ER63499 at the University of Idaho, and DE- FG07-02ER63499 at the University of Colorado.

References

Blunt, M. J., and H. Scher (1995), Pore-level modeling of wetting, *Phys. Rev. E*, *52*, 6387–6403.

Glass, R. J., and L. Yarrington (1996), Simulation of gravity-driven fingering in porous media using a modified invasion percolation model, *Geoderma*, *70*, 231–252.

Glass, R. J., and L. Yarrington (2003), Mechanistic modeling of fingering, nonmonotonicity, fragmentation, and pulsation within gravity/buoyant destabilized two-phase/unsaturated flow, *Water Resour. Res.*, *39*(3), 1058, doi:10.1029/2002WR001542.

Glass, R. J., M. J. Nicholl, and V. C. Tidwell (1995), Challenging models for flow in unsaturated, fractured rock through exploration of small scale processes, *Geophys. Res. Lett.*, *22*, 1457–1460.

Glass, R. J., M. J. Nicholl, and V. C. Tidwell (1996), Challenging and improving conceptual models for isothermal flow in unsaturated, fractured rock through exploration of small scale processes, *SAND95-1824*, 61 pp., Sandia Natl. Lab., Albuquerque, N. M.

Glass, R. J., M. J. Nicholl, and L. Yarrington (1998), A modified invasion percolation model for low capillary number immiscible displacements in horizontal rough walled fractures: Influence of local in-plane curvature, *Water Resour. Res.*, *34*, 3215–3234.

Glass, R. J., M. J. Nicholl, S. E. Pringle, and T. R. Wood (2002a), Unsaturated flow through a fracture-matrix-network: Dynamic preferential pathways in meso-scale laboratory experiments, *Water Resour. Res.*, *38*(12), 1281, doi:10.1029/2001WR001002.

Glass, R. J., M. J. Nicholl, A. L. Ramirez, and W. D. Daily (2002b), Liquid phase structure within an unsaturated fracture network beneath a surface infiltration event: Field experiment, *Water Resour. Res.*, *38*(10), 1199, doi:10.1029/2000WR000167.

Holt, R. M., R. J. Glass, J. M. Sigda, and E. D. Mattson (2003), Influence of centrifugal forces on phase structure in partially saturated media, *Geophys. Res. Lett.*, *30*(13), 1692, doi:10.1029/2003GL017340.

Ioannidis, M. A., I. Chatzis, and F. A. L. Dullien (1996), Macroscopic percolation model of immiscible displacement: Effects of buoyancy and spatial structure, *Water Resour. Res.*, *32*, 3297–3310.

Ji, S. H., I. W. Yeo, K. K. Lee, and R. J. Glass (2003), Influence of ambient groundwater flow on DNAPL migration in a fracture network: Experiments and simulations, *Geophys. Res. Lett.*, *30*(10), 1504, doi:10.1029/2003GL017064.

LaViolette, R. A., R. J. Glass, T. R. Wood, T. R. McJunkin, K. S. Noah, R. K. Podgorney, R. C. Starr, and D. L. Stoner (2003), Convergent flow observed in a laboratory-scale unsaturated fracture system, *Geophys. Res. Lett.*, *30*(2), 1083, doi:10.1029/2002GL015775.

Meakin, P., A. Birovljev, V. Frette, J. Feder, and T. Jossang (1992), Gradient stabilized and destabilized invasion percolation, *Physica A*, *191*, 227–239.

Nicholl, M. J., R. J. Glass, and S. W. Wheatcraft (1994), Gravity-driven infiltration instability in initially dry non-horizontal fractures, *Water Resour. Res.*, *30*, 2533–2546.

Su, G. W., J. T. Geller, K. Pruess, and F. Wen (1999), Experimental studies of water seepage and intermittent flow in unsaturated, rough-walled fractures, *Water Resour. Res.*, *35*, 1019–1037.

Wilkinson, D., and J. F. Willemsen (1983), Invasion percolation: A new form of percolation theory, *J. Phys. A Math Gen.*, *16*, 3365–3376.

Xu, B., Y. C. Yortsos, and D. Salin (1998), Invasion percolation with viscous forces, *Phys. Rev. E*, *57*, 739–751.

B. Andre and H. Rajaram, Civil, Environmental, and Architectural Engineering, University of Colorado, Boulder, CO 80309, USA.

R. J. Glass, Flow Visualization and Processes Laboratory, Sandia National Laboratories, Mail Stop 0735, Albuquerque, NM 87185-0735, USA. (rjglass@sandia.gov)

M. J. Nicholl, Mining and Geological Engineering, University of Idaho, Moscow, ID 83844, USA.